JOURNAL OF MATERIALS SCIENCE 28 (1993) 6650–6656

Thermal and mechanical properties of HDPE/ionomer blends

KILWON CHO*, HYUN KYOUNG JEON
Department of Chemical Engineering, Pohang Institute of Science and Technology, Pohang 790-600, Korea
TAG JIN MOON
Department of Materials Science, Korea University, Seoul 136-701, Korea

The thermal behavior, tensile and tear strength of blends containing high density polyethylene (HDPE) and a sodium neutralized ethylene–methacrylic acid copolymer ionomer have been studied. It was found that each HDPE/ionomer blend had two well-separated melting peaks and two crystallization peaks, which indicates that the components of such a blend are immiscible with each other. The tensile behavior of the ionomer showed severe strain-hardening just above the yield point, which leads to a lower elongation at break and a higher tensile strength than HDPE, possibly due to a network-like structure formation of ionic aggregates. The tensile properties of HDPE/ionomer blends were generally inferior to those of the pure components. Furthermore, the tensile properties exhibited severe negative deviation from linear additivity of properties, which is characteristic of incompatible blends. The negative deviation was also observed for tear strength of HDPE/ionomer blends. Observation of tear fracture surfaces of the blends showed fibrillar structure when ionomer content was relatively low. However, for the blends of higher ionomer composition much less fibrillation on the fracture surface was observed, which yields a higher value of tear energy. This is attributed to a network-like structure of the ionomer continuous phase of the blends.

1. Introduction

Ionomers are polymers containing a small amount of ionic salt groups attached pendantly to or in the main chain of the polymers. It is widely recognized that ionic groups in the ionomers form ionic aggregates, playing a role in physical cross-linking, resulting in substantial changes in physical properties [1–6]. Because of profound changes in physical properties, ionomers have been the subject of increasing interest from fundamental investigation to a wide range of application. Of the ionomers introduced, polyethylene-based ionomers have been used in a wide variety of applications, such as packaging films or containers, since the development of Surlyn by Du Pont in 1966 [7].

Recently, the blending of polymers has become an important approach for the development of new specialty polymers. Much work has been done on blends using polyethylene-based ionomers [8–12]. However, very limited study has been reported on blends of polyethylene and polyethylene-based ionomers [10]. Moreover, little information is available on the ultimate mechanical properties of such blends, which are important in surveying potential uses of the blends. In this paper blends containing high density polyethylene (HDPE) and a polyethylene-based ionomer are prepared and the thermal behavior and ultimate mechanical properties, such as tensile and tear strength, are investigated. Then the results are discussed with the aid of the morphology and fractography of the blends.

2. Experimental procedure

2.1. Materials

HDPE was supplied by Hanyang Chemical Company, denoted HD-9680, where the specific gravity is 0.942 and the melt flow index is 7.0 g 10 min^{-1}. The ionomer is Surlyn 1601 from the Du Pont Company. This is a random copolymer of ethylene and methacrylic acid where the acid is partially neutralized with sodium ions. The melt flow index is 1.3 g 10 min^{-1} and the specific gravity is 0.940.

2.2. Preparation of HDPE/ionomer blends

HDPE/ionomer blends having 5%, 10%, 20%, 30%, 50%, 75% and 90% by weight of ionomer with 0.1% Irganox 1010 antioxidant were prepared using a Brabender internal mixer at 160–170 °C for about 10 min. The blends were then compression-molded under a hot press and slowly cooled to room temperature.

* To whom correspondence should be addressed.

0022–2461

2.3. Thermal analysis

Differential scanning calorimetric measurements (DSC) were conducted on approximately 10 mg samples using a Perkin Elmer DSC-7. The samples were melted at 170 °C for 5 min and then quenched to room temperature at a rate of cooling of 320 °C min^{-1}, after which the melting characteristics were recorded at a heating rate of 10 °C min^{-1} to a temperature of 170 °C. After melting at 170 °C for 5 min melt crystallization temperature (T_{mc}) was measured on cooling with a cooling rate of 10 °C min^{-1}. The melting temperature (T_m) and T_{mc} were determined as the temperatures exhibiting the maximum of the peaks. The heat of fusion ΔH_f was calculated from the peak area of the endothermic peak. The degree of crystallinity was determined by ΔH_f, assuming 288.9 J g^{-1} for completely crystalline polyethylene [14].

2.4. Tensile property measurements

Thin sheets (0.5 mm thick) were prepared from the blends by compression molding at 160 °C under a hot press and slowly cooled to room temperature. Microtensile specimens of ASTM D1708 type were cut from the molded sheets. Tensile test was carried out at a crosshead speed of 10 mm min^{-1} using an Instron tensile testing machine (Model 4206) at room temperature.

2.5. Tear strength measurements

Tear test specimens, 100 mm long and 16 mm wide, were cut from the molded sheets (Fig. 1). An initial cut of about 20 mm was inserted along the center line of the specimens by means of a razor blade, thus giving a sharp tip to the initial crack. In order to minimize deviation of the tear from a linear path and to prevent gross plastic yielding at the tear tip, the groove was cut along the center line to a depth of about one-half of the total thickness, using a razor blade. The tear force F was measured at a crosshead speed of 5 mm min^{-1} using an Instron tensile test machine at room temperature. The value of tear energy G_c was calculated using the equation

$$G_c = 2F/t \quad (1)$$

where t is the tear path width measured by microscope.

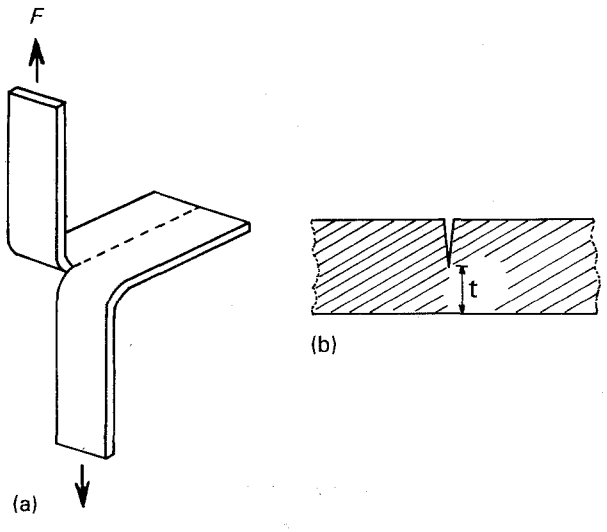

Figure 1 (a) Tear test-piece and (b) cross-section of a test-piece.

2.6. Scanning electron microscopy

The samples were fractured under cryogenic conditions using liquid nitrogen. Both the cryogenically fractured surface and the torn surface of the tear test were observed by scanning electron microscope (SEM). The sample was coated with a thin layer of gold and then examined using a Hitachi S-570 SEM operating at 15–20 kV.

3. Results and discussion

3.1. Thermal properties of the blends

The heating and cooling thermograms of various blend compositions are shown in Fig. 2 and the corresponding thermal properties are summarized in Table I. Two well-separated endothermic peaks are discernable for the blends. The sharp peak at higher temperature corresponds to the HDPE melting. The rather broad melting endotherm of the ionomer is barely detectable in the HDPE 90/ionomer 10 composition. However, the peak becomes clear with increasing ionomer content. The endothermic peak position of the HDPE appears to remain invariant while the magnitude decreases significantly with increasing ionomer content. Furthermore, no significant changes in peak position of the ionomer is observed.

In the cooling thermograms two well-separated exotherms are also clearly observed in the blends and the peak positions of each exotherm do not shift with changing composition. These results are consistent with the heating thermograms. The thermal results imply that two separate crystals are formed during crystallization of the blends, which results in immiscibility in the crystalline phases. This may be attributed to the difference in chain polarity of the two polymers, i.e. the polarity is introduced by sodium carboxylate groups into the polyethylene chains in the ionomers.

These thermal results are unexpected, because the two polymers have a very similar olefin chemical structure with only minor differences. However, on reviewing other polyolefin blends similar results were observed for LDPE/ethylene–acrylic acid copolymer blends [10], LDPE/ethylene–methacrylic acid copolymer blends [11], UHMPE/LDPE blends [15] and LLDPE/LDPE blends [16].

3.2. Morphology of the blends

The scanning electron micrographs of the cryogenically fractured surface of the HDPE/ionomer blends (Fig. 3) clearly show the two-phase structure which indicates the immiscibility of the blends. This result is consistent with that from the thermal property measurements. In the case of HDPE 70/ionomer 30 blends

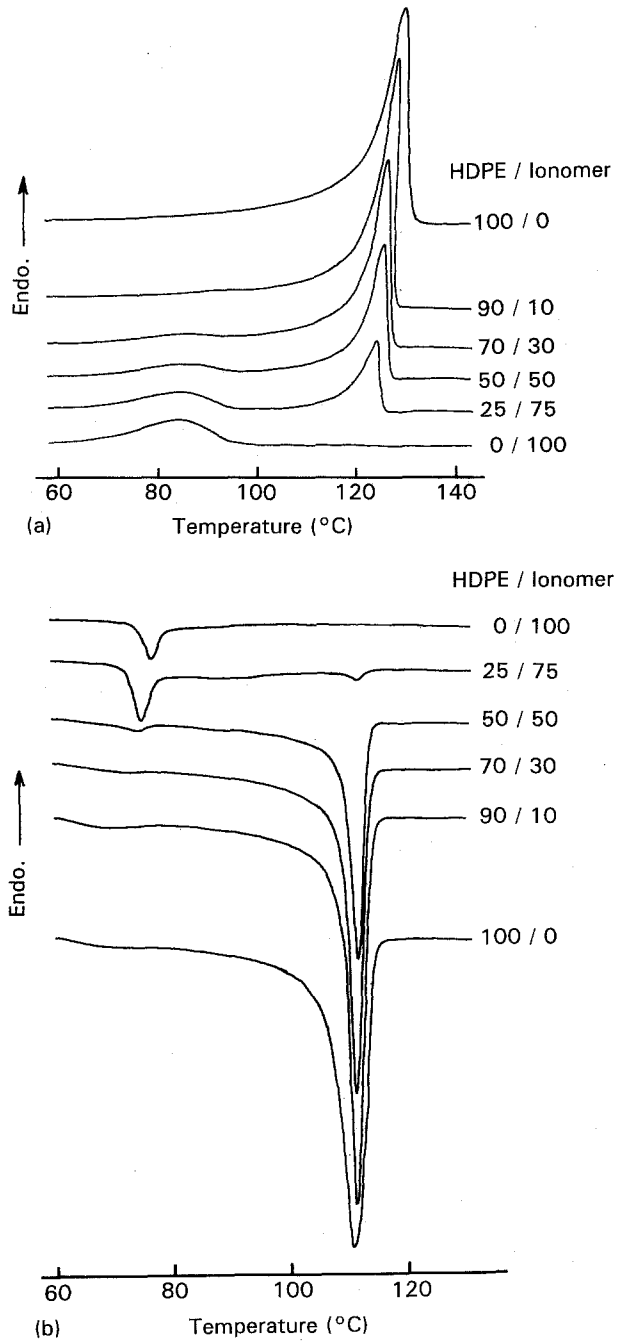

Figure 2 DSC thermograms of HDPE/ionomer blends: (a) melting behavior and (b) crystallization behavior.

the dispersed phase is ionomer and the continuous phase is HDPE. When HDPE/ionomer proportions are 50/50 the morphology looks like a co-continuous phase structure. As the ionomer content increases further phase inversion occurs and the ionomer becomes the continuous phase (Fig. 3d). The micrograph of HDPE 25/ionomer 75 reveals bimodal distribution of dispersed particle size. The large particle has a diameter of $1 \sim 2$ μm or less and the small one is around 0.2 μm in diameter. The large dispersed particle appears to have a sea-island structure.

3.3. Tensile behavior

The stress–strain curves of HDPE/ionomer blends are shown in Fig. 4. HDPE shows the typical stress–strain curve of cold-drawing semicrystalline polymers, i.e. there is a well-defined yield point, above which the tensile stress drops a little and remains almost constant as elongation proceeds then the stress rises slightly higher than the yield point until fracture eventually intervenes. However, the tensile behavior of the ionomer is quite different from that of HDPE, i.e. no cold-drawing but only strain-hardening occurs. Ionomers exhibit a yield point, however, above which the stress increases rapidly as elongation proceeds and reaches a value over twice as high as the yield point. The tensile behavior of HDPE/ionomer blends appears to be intermediate between those of HDPE and the ionomer depending on the composition of the blends. Therefore, the stress–strain behavior of HDPE/ionomer blends is much influenced by the introduction of charged polar groups such as sodium carboxylate into the blend constituents. The higher tensile strength and lower elongation of the ionomer are possibly due to the network-like structure due to physical cross-linking consisting of ionic aggregates, such as the multiplet and cluster [4, 5].

Tensile strength and elongation at break of HDPE/ionomer blends are shown in Figs 5 and 6, respectively. In the figure for elongation at break there is a minimum noted around 50 wt % ionomer composition, which is lower in magnitude than observed for the pure components. Furthermore, at all compositions the elongation at break exhibits a much lower value than the additive value, i.e. the straight line connecting the pure component values. The tensile strength also deviates negatively from a simple linear additivity relationship between properties and composition, as seen in Fig. 6. This kind of negative deviation in tensile strength and elongation at break is a characteristic of the mechanical behavior of incompatible blends with poor interfacial adhesion [17, 18].

The negative deviation in elongation at break and tensile strength is less pronounced above 50 wt % ionomer content, above which the ionomer is the continuous phase, as already seen in Fig. 3. This result implies that when the ionomer is the continuous phase the tensile properties are less affected by the addition of a small amount of the HDPE dispersed phase due to the network-like structure of ionomers.

3.4. Tear strength

The typical tear force–displacement curve of HDPE/ionomer blends is shown in Fig. 7. The tear force at first increases to a high value then drops and stabilizes, which implies stable crack growth. The high initial force is presumably required to convert the artificial crack induced by the razor blade to a natural crack associated with continuous crack propagation.

Values of tear energy G_c against blend composition for HDPE/ionomer blends are plotted in Fig. 8. For comparison of the tear energy of each composition, the thickness of the specimen was kept constant as 0.5 mm for all samples because of a strong dependence of tear energy upon thickness of the specimen [19, 20]. A quite broad minimum is observed at higher HDPE compositions in Fig. 8. Moreover, the tear energy of

TABLE I Thermal characteristics of HDPE/ionomer blends

HDPE/ionomer (wt %)	Melting temperature (°C)		Crystallization temperature (°C)		Crystallinity (%)
	$T_{m,EMA}$	$T_{m,HDPE}$	$T_{c,EMA}$	$T_{c,HDPE}$	
100/0		127.4		111.4	48.8
90/10		125.8	67.3	113.3	43.5
80/20	85.5	127.5	70.4	111.7	36.5
70/30	85.6	125.7	73.6	112.3	32.9
50/50	85.6	125.4	75.1	112.6	25.4
25/75	85.5	124.3	76.4	112.8	16.4
10/90	86.0	124.4	76.8		11.4
0/100	85.2		76.5		8.8

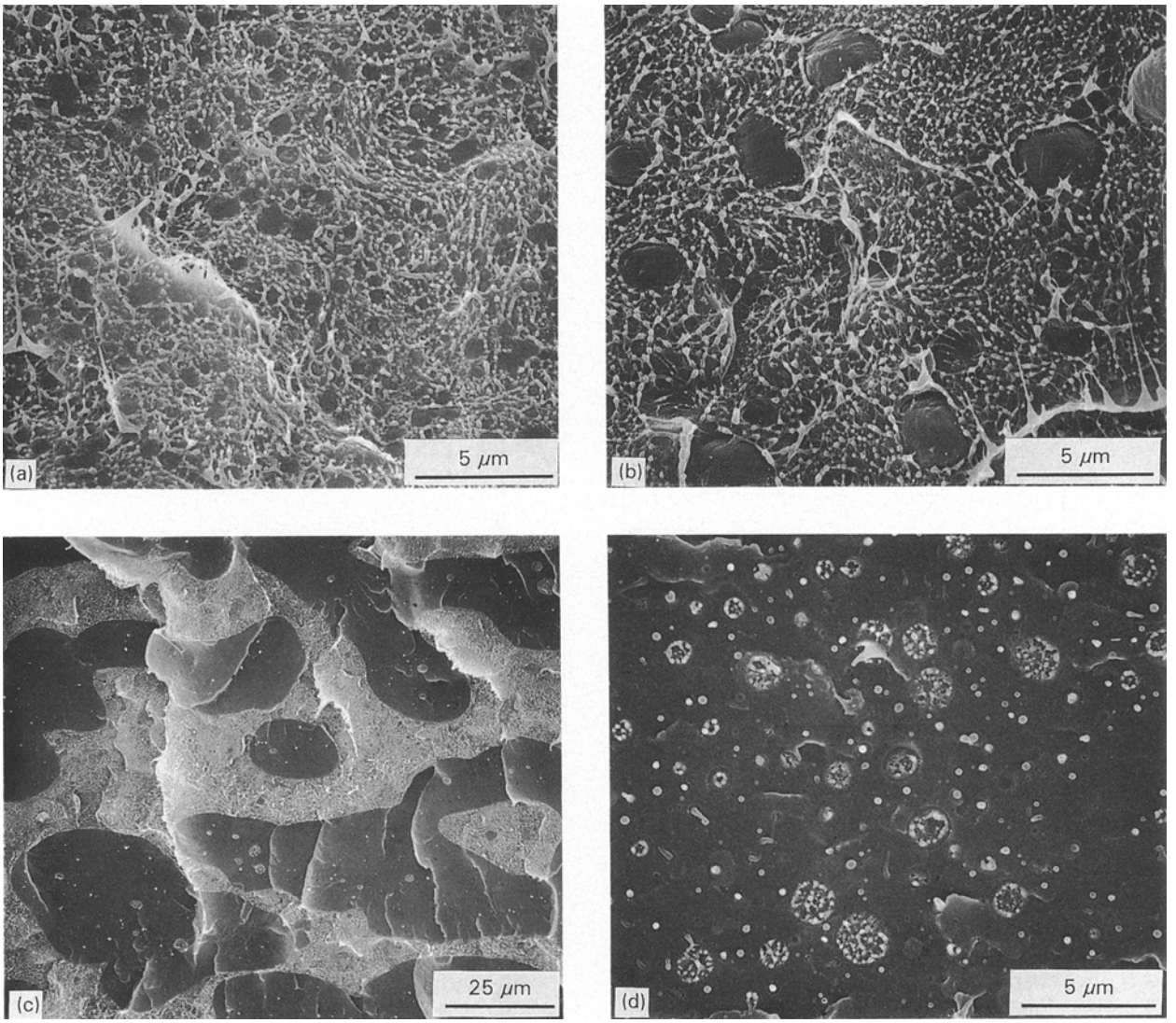

Figure 3 Scanning electron micrographs of the cryogenic fracture surface of HDPE/ionomer blends: (a) 90/10, (b) 70/30, (c) 50/50 and (d) 25/75 wt %.

the blends is considerably lower than would be expected from the additive rule of mixture, particularly at higher HDPE compositions. These results are consistent with those of the tensile test and again imply the immiscibility of HDPE/ionomer blends with poor interfacial adhesion. It is noted that tear energy decreases sharply with the addition of small amounts of ionomer, whereas above approximately 75 wt % of ionomer composition the tear energy appears to approach that of the pure ionomer. This result indicates that when the ionomer is the continuous phase the tear strength is mainly dependent upon the strength of the ionomer continuous phase due to its network-like structure, in which much energy is required to stress many bonds in order to break one strand in tearing [21]. Whereas, when HDPE is the continuous phase the ionomer dispersed particles do not enhance the strength of the HDPE continuous phase because of

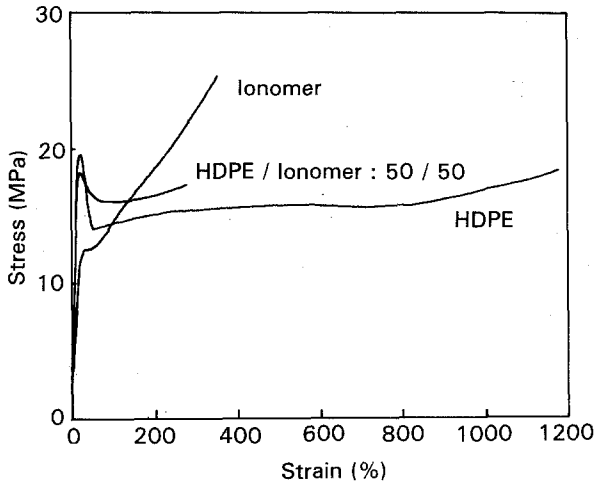

Figure 4 Stress–strain curves of HDPE/ionomer blends.

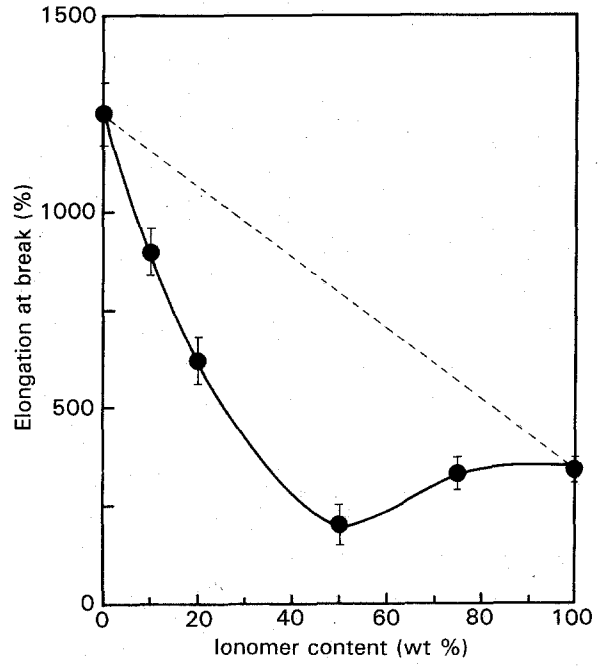

Figure 5 Elongation at break as a function of ionomer content for HDPE/ionomer blends.

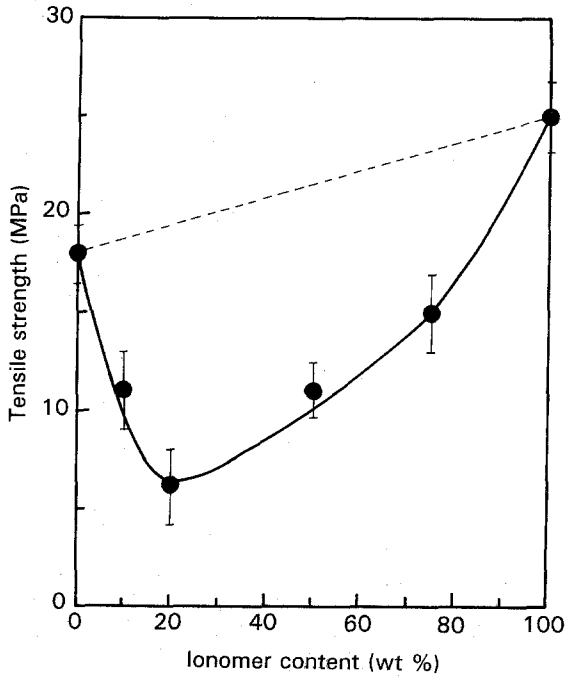

Figure 6 Tensile strength as a function of ionomer content for HDPE/ionomer blends.

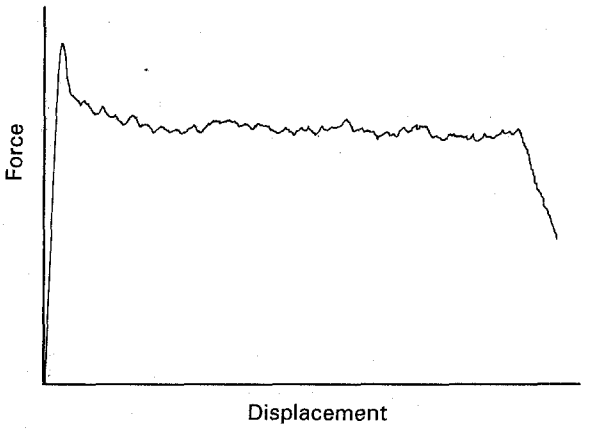

Figure 7 Typical tearing curve of HDPE/ionomer blends.

poor interfacial adhesion, which results in lower tear strength. This will be discussed in more detail in the examination of fracture surfaces.

3.5. Fractography

Scanning electron micrographs of fracture surfaces from the tear test are shown in Fig. 9. The fractograph of HDPE shows the characteristic features of ductile fracture with peaks and fibrils. The fibrils are very fine (fibril cross-section is approximately less than 0.1 μm) and maximum fibril length is about 5 μm. In the case of HDPE 70/ionomer 30 blends, the HDPE continuous phase alone is preferentially stretched, leaving the ionomer particles relatively unchanged. As a result, peaks and bundles of long fibrils are formed (maximum fibril length approximately 50 μm) and cavities are generated between the two components.

The poor interfacial adhesion between ionomer particles and HDPE continuous phases is evident from the relatively clean surfaces of the ionomer particles and the voids, as seen in Fig. 10. From this result it is regarded that the lower tear energy of blends containing below 40 wt % ionomer is associated with the two-phase morphology with a weak interface.

In contrast to the very ductile failure of HDPE, fractographs of ionomers (Fig. 9d) show wavy patterns and no fibrillar structures, which is characteristic of cross-linked elastomers [22, 23]. Actually, the ionomer has a network-like structure due to physical cross-linking by ionic aggregates [1–6]. As a result, fracture occurs by molecular chain rupture rather than viscous flow or pull-out of molecules. Thus, the network holds the structure and prevents fibrillation, which leads to a rather smooth fracture surface and a higher tear energy. These results are in close agreement with those obtained by Clements and Ward [24] for tearing of oriented polyethylene with various molecular weights, where the higher the value of fracture energy the less fibrillar is the fracture surface due to

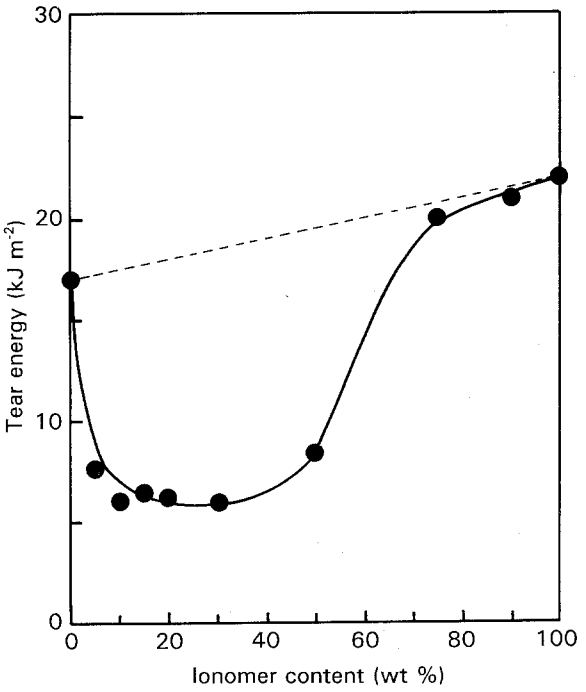

Figure 8 Tear energy as a function of ionomer content for HDPE/ionomer blends.

the formation of network-like structure by chain entanglement.

The fractograph of HDPE 25/ionomer 75 blend shows obliquely slanted sharp and fat peaks with a diameter of around 3 μm. Peaks up to 20 μm long prove ductile failure to have taken place. However, the ductility seems to be much reduced compared with the fracture surface of HDPE 70/ionomer 30 blends. This result implies that the less fibrillar structure of the fracture surface yields the higher tear energy.

4. Conclusion

The HDPE/ionomer blend is immiscible at all compositions. The tensile strength, elongation at break and tear strength of the blends exhibit negative deviation from a linear additivity of properties. The inferior mechanical behavior of the blends is attributed to the immiscibility with poor interfacial adhesion between components caused by introduction of polar groups into polyethylene chains. However, due to the network-like structure of ionomers the tear energy of the blends of relatively higher ionomer composition is little reduced. Besides, the tear fracture surface of the

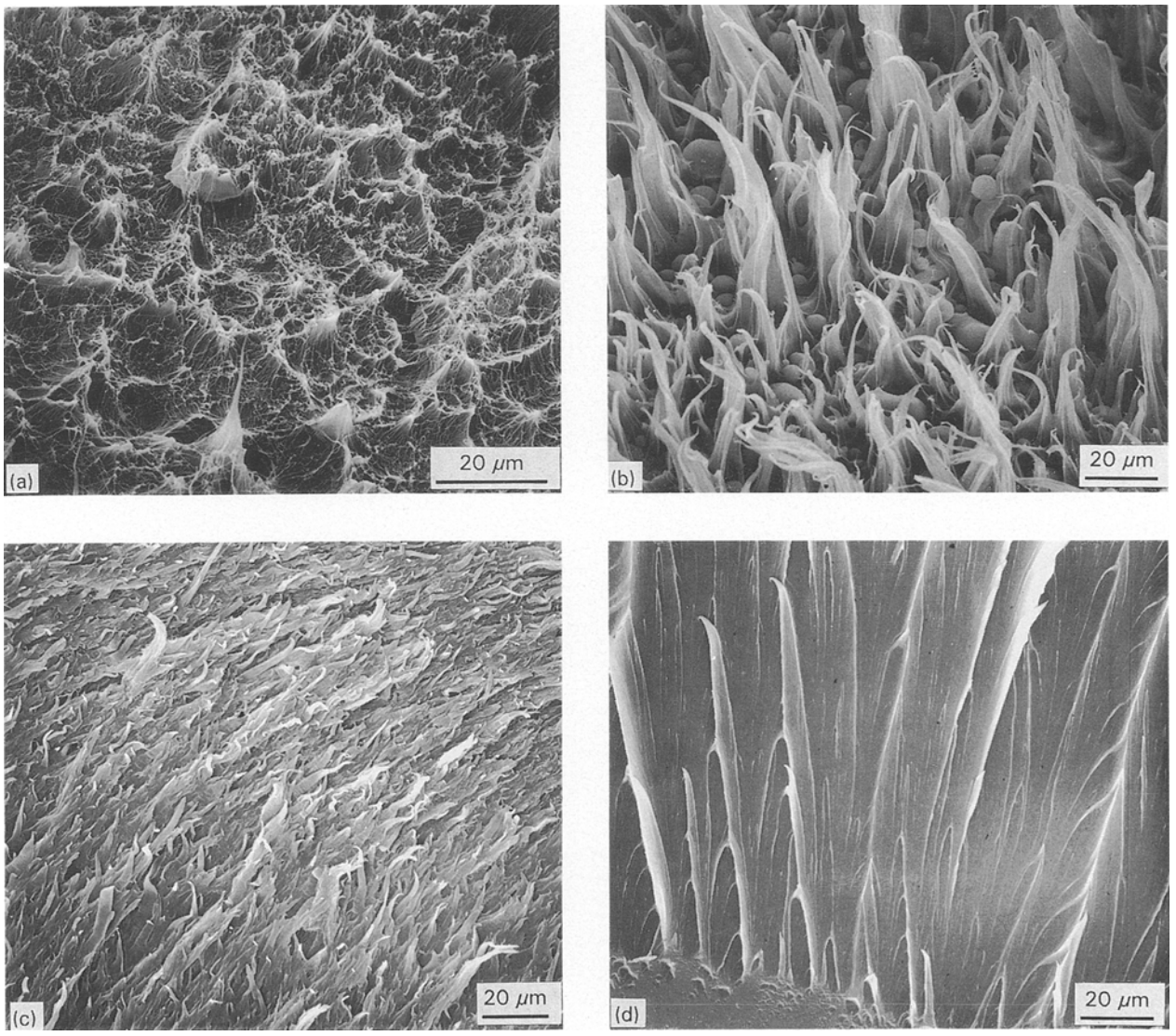

Figure 9 Scanning electron micrographs of the fracture surface from the tear test: (a) HDPE, (b) HDPE/ionomer (70/30 wt %), (c) HDPE/ionomer (25/75 wt %) and (d) ionomer.

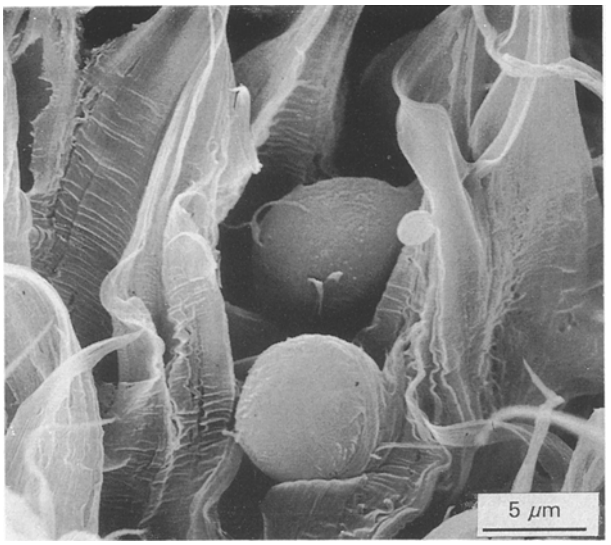

Figure 10 Higher magnification of the scanning electron micrograph of Fig. 9b, HDPE/ionomer (70/30 wt %).

ionomer has the characteristic wavy pattern of tear resistant cross-linked rubber-like materials.

Acknowledgement

This work was supported by a research grant from the Korea Science and Engineering Foundation (KOSEF 901-1005-021-2).

References

1. M. PINERI and A. EISENBERG, eds, "Structure and properties of ionomers" (D. Reidel Publishing Company, Dordrecht, Netherlands, 1987).
2. A. EISENBERG and M. KING, "Ion containing polymers" (Academic Press, New York, USA, 1977).
3. L. HOLLIDAY, ed., "Ionic polymers" (Applied Science, New York, USA, 1975).
4. W. J. MACKNIGHT and T. R. EARNEST Jr, *J. Polym. Sci. Macromol. Rev.* **16** (1981) 41.
5. E. P. OTOCKA, *J. Macromol. Sci. Rev. Macromol. Chem.* **5** (1971) 275.
6. A. D. WILSON and H. J. PROSSER, eds, "Development in ionic polymers", Vol. 1 (Applied Science, London, UK, 1983).
7. R. W. REES, US Patent 3 264 272 (1966), assigned to E. I. Du Pont de Nemours & Co.
8. V. CALDAS, G. R. BROWN and J. M. WILLIS, *Macromolecules* **23** (1990) 338.
9. J. M. WILLIS and B. D. FAVIS, *Polym Engng. Sci.* **28** (1988) 1416.
10. J. HORRION and P. K. AGARWAL, *Polym. Commun.* **30** (1989) 264.
11. G. FAIRLEY and R. E. PRUD'HOMME, *Polym. Engng Sci.* **27** (1987) 1495.
12. R. D. DEANIN, S. A. ORROTH and R. I. BHAGAT, *Polym.-Plastics Technol. Engng* **29** (1990) 289.
13. R. D. DEANIN and W. F. LIU, *Polym. Mater. Sci. Engng* **53** (1985) 813.
14. F. A. QUINN Jr and L. MANDELKERN, *J. Amer. Chem. Soc.* **80** (1958) 3178.
15. T. KYU and P. VADHAR, *J. Appl. Polym. Sci.* **32** (1986) 5575.
16. T. KYU, S. R. HU and R. S. STEIN, *J. Polym. Sci. Polym. Phys. Ed.* **25** (1987) 71.
17. D. R. PAUL, in "Multicomponent polymer materials", Advances in Chemistry Series No. 211, edited by D. R. Paul and L. H. Sperling (ACS, Washington, DC, USA, 1986) p. 3.
18. E. PERRY, *J. Appl. Polym. Sci.* **8** (1964) 2605.
19. R. P. KAMBOUR and S. MILLER, *J. Mater. Sci.* **11** (1976) 823.
20. D. S. CHIU, A. N. GENT and J. R. WHITE, *ibid.* **19** (1984) 2622.
21. G. J. LAKE and A. G. THOMAS, *Proc. R. Soc. Lond. A.* **A300** (1967) 108.
22. A. E. WOODWARD, in "Atlas of polymer morphology" (Hanser Publishers, Munich, Germany, 1988) p. 459.
23. L. ENGEL, H. KLINGELE, G. W. EHRENSTEIN and H. SCHAPER, eds, "An atlas of polymer damage" (Wolfe Science Books, Munich, Germany, 1986) p. 137.
24. J. CLEMENTS and I. M. WARD, *J. Mater. Sci.* **18** (1983) 2484.

Received 3 August 1992
and accepted 4 January 1993